Influence of Anodized Titanium Surfaces on the Behavior of Gingival Cells in Contact with: A Systematic Review of In Vitro Studies

Marie-Joséphine Crenn, Pierre Dubot, Elie Mimran, Olivier Fromentin, Nicolas Lebon, Patrice Peyre

crystals

MDPI

Systematic Review

Influence of Anodized Titanium Surfaces on the Behavior of Gingival Cells in Contact with: A Systematic Review of In Vitro Studies

Marie-Joséphine Crenn [1,2,*], Pierre Dubot [3], Elie Mimran [2], Olivier Fromentin [2], Nicolas Lebon [4] and Patrice Peyre [1]

1 CNRS-Arts et Métiers ParisTech UMR 8006, Laboratoire Procédés et Ingéniérie en Mécanique et Matériaux (PIMM), 75013 Paris, France; patrice.peyre@ensam.eu
2 UFR d'Odontologie Garancière, Université de Paris, 75006 Paris, France; eliemimran@gmail.com (E.M.); olivier.fromentin@univ-paris-diderot.fr (O.F.)
3 Institut de Chimie et des Matériaux de Paris-Est (ICMPE), CNRS-Université Paris-Est UMR 7182, 94320 Thiais, France; pdubot@glvt-cnrs.fr
4 UR 4462, Unité de Recherche en Biomatériaux Innovants et Interfaces (URB2i), 92120 Montrouge, France; lebon@univ-paris13.fr
* Correspondence: marie-josephine.crenn@univ-paris-diderot.fr

Abstract: Electrochemically anodized (EA) surfaces promise enhanced biological properties and may be a solution to ensure a seal between peri-implant soft tissues and dental transmucosal components. However, the interaction between the modified nano-structured surface and the gingival cells needs further investigation. The aim of this systematic review is to analyze the biological response of gingival cells to EA titanium surfaces in in vitro studies with a score-based reliability assessment. A protocol aimed at answering the following focused question was developed: "How does the surface integrity (e.g., topography and chemistry) of EA titanium influence gingival cell response in in vitro studies?". A search in three computer databases was performed using keywords. A quality assessment of the studies selected was performed using the SciRAP method. A total of 14 articles were selected from the 216 eligible papers. The mean reporting and the mean methodologic quality SciRAP scores were 87.7 ± 7.7/100 and 77.8 ± 7.8/100, respectively. Within the limitation of this review based on in vitro studies, it can be safely speculated that EA surfaces with optimal chemical and morphological characteristics enhance gingival fibroblast response compared to conventional titanium surfaces. When EA is combined with functionalization, it also positively influences gingival epithelial cell behavior.

Keywords: dental abutment; anodic oxidation; titanium; TiO_2 nanotubes; human gingival fibroblasts

Citation: Crenn, M.-J.; Dubot, P.; Mimran, E.; Fromentin, O.; Lebon, N.; Peyre, P. Influence of Anodized Titanium Surfaces on the Behavior of Gingival Cells in Contact with: A Systematic Review of In Vitro Studies. *Crystals* **2021**, *11*, 1566. https://doi.org/10.3390/cryst11121566

Academic Editor: Abel Moreno

Received: 12 November 2021
Accepted: 11 December 2021
Published: 15 December 2021
Corrected: 24 June 2022

1. Introduction

Soft tissue integration is currently a major challenge in implant-prosthetic treatment. Although during the last decade, osteointegration has been the major topic of interest in enhancing the implant survival rate [1], recently, attention has shifted to the barrier formed between the soft tissues and the surface of the transmucosal component. Indeed, stabilizing the connective tissue and the epithelial attachment on the abutment surface (in the case of a bone-level implant) or on the implant neck (in the case of a tissue-level implant) is now considered as the key to safeguarding the implant from bacterial contamination and thus reducing the risk of peri-implantitis [2]. Further techniques have been proposed to promote the surface bioactivity of Ti surfaces, such as mechanical modifications (sandblasting, acid-etching, micro-grooving), physical modification (laser), chemical modifications, and biological coating (proteins, collagen, hydroxyapatite, nanoparticles). Among these modifications, nano-engineered surfaces have gained interest by mimicking the extracellular matrix substrates. Several methods have been described to obtain a nanotextured

surface, but electrochemical anodization or anodic oxidation is considered the most popular cost-effective approach to creating a nano-structured TiO_2 oxide layer [3]. This technique, which consists of the immersion of the target piece in an appropriate electrolyte, was shown to establish a specific nano-structured surface due to the current created between the target metallic piece (anode) and another metal (cathode) through the application of a voltage (Figure 1).

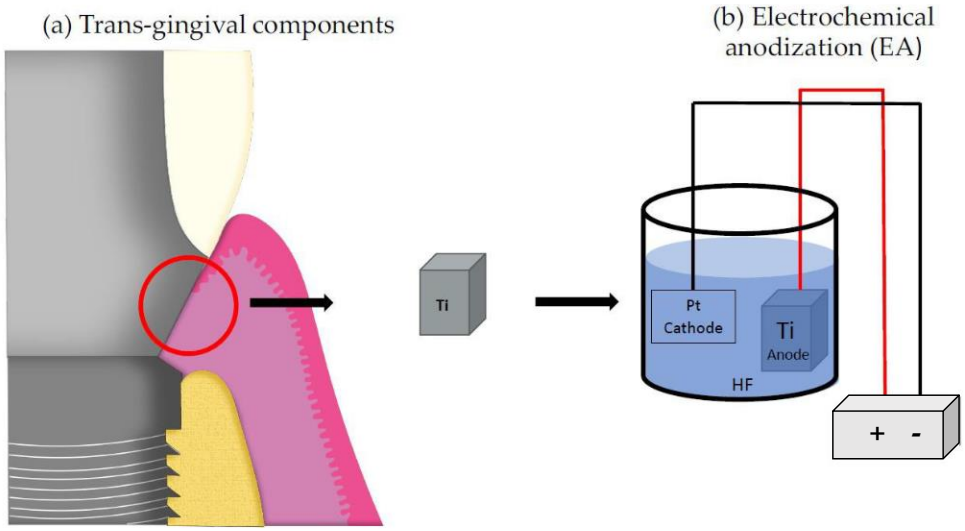

Figure 1. Schematic representation of (**a**) the trans-gingival abutment-mucosa interface and (**b**) the electrochemical anodization step to fabricate TiO_2 nanotubes or nanopores.

This specific nano-featured surface is characterized by the presence of nanopores (NP) or nanotubes (NT) whose morphology (diameter, length, wall thickness) and surface chemistry (crystallinity) vary according to the experimental conditions [4] (Figure 2).

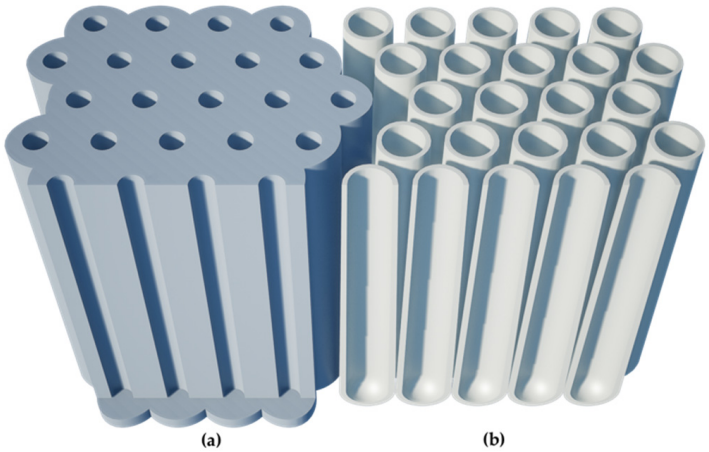

Figure 2. Schematic representation of (**a**) of nanopores NP and (**b**) nanotubes.

It is well known that cell behavior is sensitive to surface characteristics such as chemical and physical features [5] and to surface topography and surface reactivity, also EA seems to enhance fibroblast/epithelial response and cell functions. This trend was highlighted by the first in vitro studies investigating fibroblast and epithelial cell response on anodized titanium surfaces [1,6]. However, due to the lack of reproducibility, it remains very difficult to understand the real impact of these surface characteristics on the soft tissue's response. Although in vitro studies cannot explain the complex interactions which occur in the human body, it remains an interesting investigation since it allows precise understanding of the influence of one parameter on a cell line.

The purpose of this systematic review is to investigate, with a score-based reliability evaluation, how the surface properties of anodized titanium surfaces influence the cellular response of gingival cells, in order to enrich the discussion of existing literature about the optimization of such surfaces for trans-gingival components.

2. Materials and Methods

2.1. Protocol

The present systematic review is reported in accordance with the guidelines of Transparent Reporting of Systematic Reviews and Meta-Analyses (PRISMA statement) [7].

The focusing question was: "How does the surface integrity (such as topography and chemistry) of the anodized titanium influence the cellular response of gingival cells in in vitro studies?".

A detailed protocol following the PICO (Population-Intervention-Comparison and Outcomes) strategy was designed to answer this question.

- Population: In vitro studies analyzing fibroblastic and epithelial cell response (since they are both the main resident cell populations in the peri-implant connective attachment) to different electrochemical anodized (EA) titanium surfaces.
- Intervention: Surface modification, known as "anodic oxidation", which creates a nanofeature surface.
- Comparison: Titanium surfaces obtained in the same conditions as the treated on, but without EA.
- Outcomes: Cellular response with a minimum requirement of a qualitative and/or quantitative adhesion evaluation.

The inclusion criteria were:

- In vitro studies.
- Studies investigating gingival fibroblasts and epithelial cell response to anodized titanium surfaces with nanotubes or nanopores.
- Studies including in their protocol any supplementary modifications previous EA or following EA.

The following studies were excluded:

- Studies proposing a surface modification protocol other than anodic oxidation on a titanium alloy.
- Studies investigating the response of cells different from fibroblasts and epithelial cells (e.g., osteoblasts or bacterial cells).
- Studies investigating soft tissue response in vivo.
- Anodization protocol that does not induce a nanopore or nanotube type nano-structured surface.
- Studies that do not detail the anodization parameters.
- Studies without qualitative or quantitative assessment of cell adhesion/attachment.
- Studies that did not provide information on the morphology of nanotubes/nanopores.

2.2. Search Strategy

An electronic restricted search of studies published only between 1 January 2011 and 31 December 2020 in three databases (MEDLINE/Pubmed, EMBASE, and Web of Sciences) was performed using keywords related to anodization on titanium surfaces combined with keywords related to soft tissues with AND/OR as Boolean operators. This equation was structured as shown in Table 1. No limits were applied regarding the sample size, but only articles written in English were selected.

Table 1. Search strategy and keywords.

(1) "anodic oxidation" OR "surface modification*" OR "modified surface*" OR "anodization" OR "nano topography" OR "anodized" OR "nanotube*"
(2) "abutment*" OR "dental abutment*" OR "dental implant*"
(3) "fibroblast*" OR "human gingival fibroblast*" OR "gingival cell*" OR "peri-implant soft tissue*" OR "gingival epithelial cell*"
(4) "titanium" OR "titanium alloy*" OR "Ti6Al4V"
(5) "Zirconia" OR "Zirconium"
1 AND 2 AND 3 AND 4 NOT 5

The results of the electronic research were imported into software (Excel, Microsoft) to exclude duplicates. Titles and abstracts were screened by two independent reviewers (MJC and EM). Irrelevant studies unrelated to the response of gingival soft tissues on anodized nano-structured titanium surfaces were excluded. In case of difference, a consensus was decided by a supervisor (OF). To improve the sensitivity of the search, the references of all the papers included in the systematic review were checked to potentially reveal additional studies. Then, the full texts of all potentially eligible papers were assessed according to inclusion criteria. The inclusion or exclusion of studies was decided independently by the two reviewers (MJC and EM). In case of difference, a consensus was also decided by the supervisor (OF).

2.3. Data Extraction and Analysis

Data were extracted independently by the two reviewers using two tables specifically developed for this purpose. The first table included the article title and year of publication, sample preparation (materials, fabricant, and anodization parameters), and biological evaluation (measuring variables, methodology, cell density, duration, and number of replicates). The second table presented the characteristics of the different surfaces (surface roughness, NT/NP morphology, and wettability) and the biological results compared to the control surface.

2.4. Quality Assessment of Individual Studies

As described in Corvino et al., 2020 [1], a quality assessment of the selected studies was performed following the SciRAP method (http://www.scirap.org, accessed on 1 September 2021). Briefly, SciRAP is a webtool method developed to evaluate both the reliability and the relevance of in vitro studies. Regarding reliability, the criteria used to evaluate "reporting quality" (n = 23) and "methodological quality" (n = 15) separately can be adopted in the evaluation of studies focusing on the cellular response on biomaterials. However, the criteria (n = 4) used for the evaluation of relevance are strictly related to the evaluation of studies on toxicity for the assessment of human health hazards or risks. Therefore, these criteria cannot be taken into account to evaluate the quality of the in vitro studies selected in this review. Other criteria can be selected as "fulfilled", "partially fulfilled", or "not fulfilled". The final score for each category can range between 0 and 100, where 100 is the situation for which all the criteria are judged "fulfilled". For all the studies, three criteria were removed from the reporting quality evaluation and four from the methodological quality evaluation because they were applicable only for the evaluation of the soluble tested component.

3. Results and Discussion

3.1. Search and Included Studies

From the initial search, 216 potential articles were found through database searching. After reading the titles and abstracts, 169 were excluded, and after reading the full-text articles, 33 articles were eliminated. A total of 14 articles were included for qualitative synthesis (Figure 3).

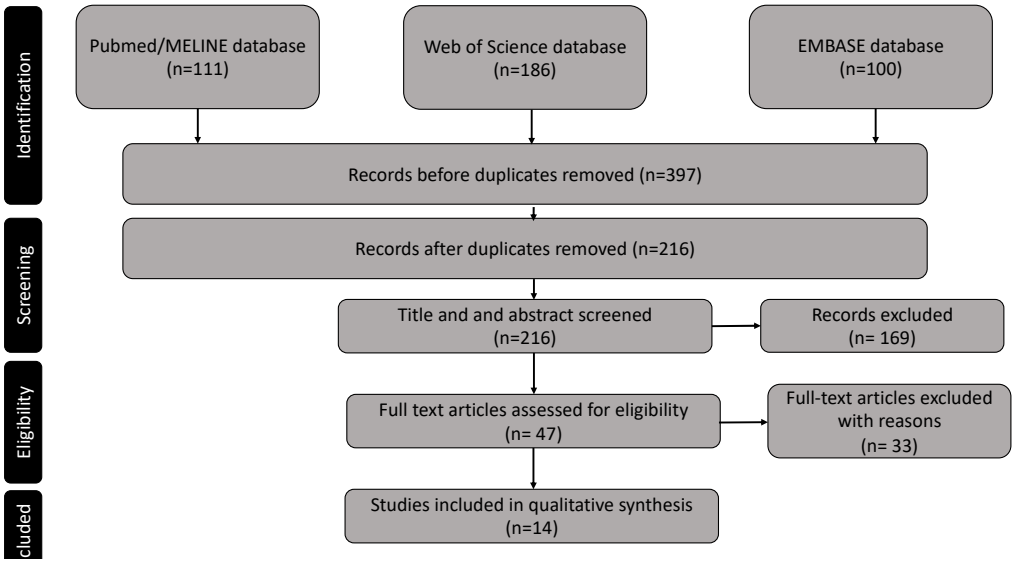

Figure 3. Flow chart depicting the selection process.

3.2. Quality Assessment of the Included Studies

According to previous systematic reviews of in vitro studies, the quality of the studies was evaluated by the SciRAP method (Figure 4).

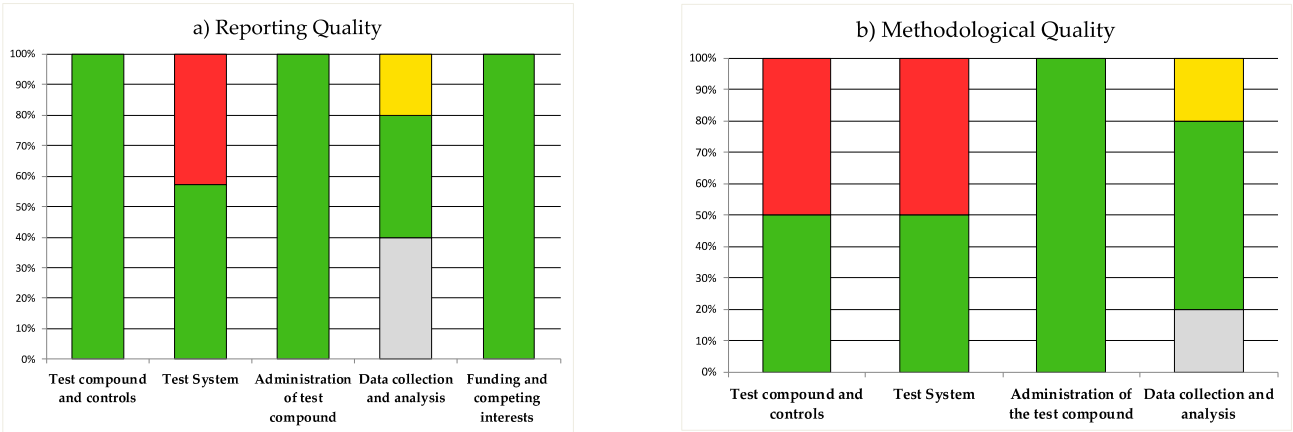

Figure 4. An example of a color profile generated with the SciRAP tool. In the color profile, the evaluation of (**a**) reporting quality and (**b**) methodological quality are illustrated in bar charts, showing green for fulfilled criteria, yellow for partially fulfilled criteria, and red for criteria that were not fulfilled.

All the included studies defined a machined or polished titanium surface as a control surface. All the included studies described the cell density for the evaluation of proliferation but not systematically for the analysis of other cell functions. A total of 11 out of 14 studies reported the manufacturer of the tested titanium materials. All the included studies clearly defined the tested cell lines (source), although not all specified the number of passages. Additionally, 8 studies described how they sterilized the samples before tests, and 11 detailed the number of replicates for each test. No calculation of the sample size was described, and only a few studies verified normality before performing the statistical test.

The mean reporting quality score was 87.7 $\pm$ 7.7/100 while the mean methodologic quality score was 77.8 $\pm$ 7.8/100. Details of quality evaluations are shown in Table 2.

Table 2. Reporting and methodological quality score of the studies included calculated with the SciRAP method.

		SciRAP Score		
		Reporting Quality	**Methodologic Quality**	**Ref.**
1	Wang et al., 2020	90	80	[8]
2	Gulati et al., 2020	95	80	[9]
3	Xu et al., 2020	80	70	[10]
4	Zheng et al., 2020	80	80	[11]
5	Llopis Grimalt et al., 2019	77.7	75	[12]
6	Wang et al., 2019	92.5	85	[13]
7	Ferrà-Cañellas et al., 2019	92.5	95	[14]
8	Nojiri et al., 2019	82.5	80	[15]
9	Gulati et al., 2018	72.5	65	[16]
10	Xu et al., 2018	97.5	80	[17]
11	Liu et al., 2014	87.5	70	[18]
12	Guida et al., 2013	95	85	[19]
13	Ma et al., 2012	92.5	70	[20]
14	Ma et al., 2011	92.5	75	[21]

3.3. Characteristics of the Included Studies

After full-text article reading, a meta-analysis was not possible given the extreme heterogeneity in these studies' designs and measurement parameters.

Table 3 summarizes the main characteristics of the reviewed studies. Pure titanium was the most common material used [8,9,13,14,16,18–21]. Some studies included grade 2 or 4 titanium [11,12,15,17], but none of them proposed a protocol including grade 5 titanium, which is generally the titanium alloy used for trans-gingival components.

Anodization parameters differed for each study. All the included studies systematically described the voltage, the anodization time, and the nature and composition of the electrolyte. One study highlighted the role of the distance between the cathode and the anode [14]. Two studies also described the importance of the age of the electrolyte [9,14] used specifically to conserve the underlying microroughness of a titanium substrate [22]. Little information was provided on the temperature of the bath, although the temperature can influence the viscosity of electrolytes. Platinum was the material most reported for cathodes, although one study used copper [15].

The choice of sterilization methods was described in 8 studies, whereas it can affect the biocompatibility of the TiO_2 surface. UV irradiation was chosen in 5 studies [9,10,16,20,21] and appears to be the most appropriate technique since it maintains the bioactivity of the nanostructure [23,24].

The voltages imposed were between 10 V [10] and 80 V [9,16]. The electrolytes were almost all composed of a viscous mixture (based on glycerol or ethylene glycol) and water. The presence of fluoride ion F- was observed systematically, either as NH_4F or HF at a concentration of approximately 0.5% [8,10,11,13,17,20,21]. In contrast, some protocols included less F-content: 0.3% [9,16], 0.15% [19], or more 1% [18]. Four studies resulted in the formation of a surface with nanopores (NP) [9,12,14,16] and ten studies resulted in the formation of nanotubes (NT) [8,10,11,15,17–21,23]. Generally, the studies proposing a "short" anodization protocol with a time less than 30 min and the presence of a low amount of F- resulted in NP features. On the other hand, with over 30 min of anodization and with a fluoride ion concentration of 0.5%, most of the studies showed the formation of well-defined, organized NT. One study showed that a rippled rough surface without NT or NP was obtained [15] under conditions with a lower voltage (1 V, 5 V, 10 V).

Table 3. Main characteristics of the studies reviewed.

Study/Year	Sample Preparation			Bioactivity Evaluation		
	Materials and Fabricant	**Anodization:** **- Applied Voltage** **- Anodization Time** **- Electrolyte Composition**	**Cell Line (Type, Source, Number of Passages)**	**Sterilization before Testing**	**Analyzed Functions, Methodology, Cell Density (or Number of Cells) and Duration of Treatment**	**Number of Replicates**
Wang et al., 2020	Pure titanium Cuibolin Nonferrous Metal Industry Co., Ltd., (Beijing, China).	• 50 V • 15 min • Ethylene glycol + 0.5 wt% NH4F + 10 vol% DW	hGF from collections Passage: 2–6	NS	• Cell adhesion by the CCK − 8 assay (1×10^4 cells/well) at 1, 2, and 4 h • Cell proliferation by the CCK − 8 assay (5×10^4 wells/well) at 1,3,5 and 7 d • Cell morphology by SEM (1×10^4 cells/well) at 1, 4, and 24 h • Focal adhesion after VCL/DAPI staining and observation by confocal laser scanning microscopy (1×10^4 cells/well) at 4 and 24 h • Migration by a wound − healing assay (1×10^5 cells/well) at 12 and 24 h • Gene expression of adhesion-related proteins (FAK, ITGα2, ITGβ1, VCL, FN1) and ECM components (COL-1A1) by Rt-qPCR at 4 and 24 h • Type I collagen and fibronectin synthesis by ELISA at 1,4 and 7 d	n = 3 at least
Gulati et al., 2020	Pure titanium Nilaco, (Tokyo, Japan).	• 40 V; 60 V; 80 V. • 10 min • Ethylene glycol + 0.3 wt% NH4F + 1% *v/v* DW	Primary hGFs Passage: 4	UV irradiation for 1 h each side	• Cell adhesion by calculations of morphology parameter at 1, 6 h, 1, and 3 d • Cell viability by Alamar Blue assay (1×10^4 cells/well) at 1,3 and 7 d • Cell morphology by SEM at 1 h to 7 d • Gene expression of adhesion-related proteins (FN, ITGβ1, ICAM-1), ECM components (COL-1, COL-3) and growth factor by Rt-qPCR (VEGF) at 1,3 and 7 d	n = 3
Xu et al., 2020	Titanium NS NS	• 10 V; 30 V; 60 V • 3 h • Glycerol (1,2,3-propanetriol) + 0.5 wt% NH4F + 10 vol% DW	hGF from biopsies	UV irradiation for 30 min each side	• Cell adhesion after DAPI staining and analysis by fluorescence intensity (4×10^4 cells/well) at 2 h • Cell proliferation by the CCK − 8 assay (2×10^4 cells/well) 1,3,7 d • Cell morphology by SEM at day 2 (2×10^4 cells/well) at 2 d • Gene expression of adhesion-related proteins (FN, ITGβ1, VCL) and ECM components (COL-1) by Rt-qPCR (VEGF) at 1,3 and 7 d	n = 3
Zheng et al., 2020	Titanium grade IV Baoji Titanium Industry Co., Ltd. (Shaanxi, China)	• 30 V • 4 h • Glycerol (1,2,3-propanetriol) 50% + 0.27 M NH4F + 50 vol% DW	hGF from collection	NS	• Cell adhesion after DAPI staining and analysis by fluorescence intensity (2×10^4 cells/well) at 4 h and 24 h • Cell proliferation by CCK-8 at 1, 3, 5, and 7 d • Migration by a wound-healing assay at 24 h • Gene expression of adhesion − related proteins (FN, FAK) by RT − qPCR ($1\times$ 106 cells/well) at 24 h • Phosphorylated-FAK and fibronectin expression by western blot analysis at 24 h	NS

Table 3. *Cont.*

Study/Year	Sample Preparation		Bioactivity Evaluation			
	Materials and Fabricant	**Anodization:** **- Applied Voltage** **- Anodization Time** **- Electrolyte Composition**	**Cell Line (Type, Source, Number of Passages)**	**Sterilization before Testing**	**Analyzed Functions, Methodology, Cell Density (or Number of Cells) and Duration of Treatment**	**Number of Replicates**
Llopis-Grimalt et al., 2019	Titanium grade IV Implantmedia (Lloseta, Spain)	• 35 V; 60 V • 30 min and 10 min • Ethylene glycol + 0.1 M NH4F + 8 M or 1 M DW	hGF from biopsies	NS	• Cell adhesion by Presto Blue reagent at 30 min • Cytotoxicity analysis by LDH activity at 48 h • Cell proliferation by Presto Blue reagent at 2,7 and 14 d • Collagen quantification after staining and absorbance at 14 d • Cell orientation after DAPI/FITC staining and observation by confocal laser scanning microscopy; duration: NS	NS
Nojiri et al., 2019	Titanium grade II Gallium Source (LLC, CA, USA).	• 30 V • 3 h • Ethylene glycol + 0.28 vol% NH4F + 1.79 vol% DW	hGEC from collection	NS	• Cell adhesion by the CCK − 8 assay (1×10^5 cells/cm^2) at 3 h • Cell adhesion by SEM at 3 h	n = 3
Wang et al., 2019	Pure titanium Northwest Institute for Nonferrous Metal Research (Xi'an, China)	• 20 V • 30 min • DW + 0.5% HF	hGEC from biopsies Passage: 2–5	NS	• Cell adhesion after DAPI staining and analysis by fluorescence intensity at 4 h (1×10^4 cells/well) • Cell morphology by SEM at 2, 6, 12 h and 3 d (1×10^4 cells/well) • Cell viability by CCK − 8 at 4 h, 1, 3, 5 and 7 d (1×10^4 cells/well) • Observation of the cellular uptake of pLAMA3 − CM by HEGCs by confocal laser scanning microscopy at 48 h (1×10^4 cells/well) • Gene expression of adhesion − related proteins at 48 h (LAMA3, ITGβ4) by RT − qPCR (1×10^6 cells/well) • Protein synthesis (LAMA3, ITGβ4) by fluorescence intensity at 3 d (1×10^4 cells/well)	n = 6
Ferra-Canellas et al., 2018	Pure titanium Sigma-Aldrich (St-Louis, MO, USA).	• 35 V-1 V; 60 V • 30 min and 10 min. • Ethylene glycol + 0.1 M NH4F + 1 M DW	hGF from biopsies Passage: 9 and 7	NS	• Cell adhesion by Presto Blue reagent at 30 min • Cytotoxicity analysis by LDH activity at 48 h • Cell proliferation by Presto Blue reagent at 7 and 14 d • Gene expression of proteins at 14 d (COL − 1, COL − 3, DCN) by RT − qPCR (1×10^6 cells/well) • Collagen quantification after staining and absorbance at 14 d	n = 6 or 3depends on the test
Xu et al., 2018	Titanium grade II Western BaoDe (Xi'an, PR China)	• 20 V • 45 min • DW + 0.5% wt% HF	hGF from biopsies Passage:5 and 8hGEC from biopsies Passage: 2 et 4	Autoclave sterilized	• Cell adhesion by SEM at 24 h (1×10^4 cells/mL) • Cell morphology by SEM at 24 h (1×10^4 cells/mL) • Cell proliferation by CCK − 8 at 1, 3, 5, and 7 d (1×10^4 cells/mL) • Gene expression of adhesion − related proteins (ITGα6, ITGβ4, LAMA3, LAMB3, LAMG2 for hGEC and ITGα3, ITGβ1, FN and VCL for hGF) and ECM components by RT − qPCR at 7 d (5×10^4 cells/mL) • Type I collagen synthesis (for hGF) and hEGF protein secreted (for hGEC) synthesis by ELISA at 1, 2 and 4 d (5×10^4 cells/mL)	n = 3

Table 3. *Cont.*

Study/Year	Sample Preparation				Bioactivity Evaluation	
	Materials and Fabricant	**Anodization:** **- Applied Voltage** **- Anodization Time** **- Electrolyte Composition**	**Cell Line (Type, Source, Number of Passages)**	**Sterilization before Testing**	**Analyzed Functions, Methodology, Cell Density (or Number of Cells) and Duration of Treatment**	**Number of Replicates**
Gulati et al., 2018	Pure titanium Nilaco, (Tokyo, Japan).	• 60 V, 80 V • 10 min, 15 min • Ethylene glycol + 0.3 wt% NH4F + 1% *v/v* DW	Primary hGF	UV irradiation for 1 h each side	• Cell proliferation by the CCK − 8 assay at 1, 4 and 7 d (5×10^4 cells/well) • Cell morphology by SEM at 24 h 1, 4 and 7 d (5×10^4 cells/well)	n = 3
Liu et al., 2014	Pure titanium NS	• From 0 to 25 V at 500 mV/s and kept at 25 V • 1 h • Glycerol (1,2,3-propanetriol) + 1.0 wt% NH4F + 15 vol% DW	hGF from collection Passage: 3–5	Ozone for 30 min	• Cell adhesion after DAPI staining and analysis by fluorescence intensity at 1 and 3 h • Cell proliferation by the MTS assay kit at 3, 4, 7, and 14 d • Cell morphology by SEM at 1, 3, 9 and 24 h (2×10^4 cells/cm^2) • Gene expression of ECM protein (COL-1) by FQ-PCR at 3, 4, 7, and 14 d • Type I collagen synthesis by ELISA at 3, 4, 7, and 14 d	NS
Guida et al., 2013	Pure titanium P.H.I s.r.l (San Vittore Olana, Milano, Italy)	• 20 V • 24 h • DW + 0.15% HF + 1 M sulfuric acid	hGF from biopsies Passage: between 2 and 4	Autoclave sterilized	• Cell adhesion by MTT assay at 6 h (30.000 cells/cm^2) • Cell proliferation by MTT assay at 48 h and 7 d (30.000 cells/cm^2) • Cell morphology by SEM at 6 h and confocal laser scanning microscopy after staining at 24 h • Type I collagen synthesis by ELISA at 6, 48 h, and 7 d	All experiments were performed 2 times in triplicate on 2 different cell preparations
Ma et al., 2012	Pure titanium Northwest Institute for Nonferrous Metal Research (Xi'an, China)	• 20 V • 45 min • DW + 0.5% NH4F + 1 M ammonium sulfate	hGF from biopsies Passage: 4	UV irradiation for 2 h	• Cell adhesion by confocal laser scanning microscopy after DAPI staining at 30, 60, 120 min (1×10^5 cells/mL) • Cell proliferation by MTT assay at 1, 3, 6 and 9 d (4×10^4 cells/well) • Cell morphology by SEM at 3 d • Gene expression of ECM protein by RT-qPCR at 3, 6 and 9 d (VEGFA, ITGβ, ICAM1, LAMA1)	n = 3
Ma et al., 2011	Pure titanium NS	• 20 V • 45 min • DW + 0.5 vol% NH4F + 1 M ammonium sulfate	hGF from biopsies Passage: 4 L292 cells	UV irradiation for 2 h	• Cytotoxicity analysis by MTT at 24, 48, and 72 h • Cell adhesion by confocal laser scanning microscopy after DAPI staining at 30, 60, 120 min (1×10^5 cells/mL) • Cell proliferation by MTT assay at 3, 6 and 9 d (4×10^4 cells/well) • Gene expression of ECM protein by RT-qPCR at 3, 6 and 9 d (COL-1, COL-3, VEGFA, ITGβ, FN, ICAM1)	n = 3

Abbreviations: HF: hydrofluoric acid; NH4F: ammonium fluoride; DW: deionized water; Rt-qPCR: reverse transcription-quantitative real-time polymerase chain reaction; SEM: scanning electron microscope, CCK-8 assay: cell counting kit-8 assay; hGF: human gingival fibroblast; hGEC: human gingival epithelial cell, CCK-8: Cell Counting Kit-8 assay; MTS: methyl tetrazole sulfate; VCL: vinculin; COL-1: collagen 1; COL-3: collagen-3; ITGα2: integrin α2; ITGβ1: integrin β1; ITGβ4: integrin β4; FAK: focal adhesion kinase; FN: fibronectin; DAPI: 4′,6-diamidino-2-phenylindole; FITC: phalloidin-fluorescein isothiocyanate; LAMA: laminin-5 α3; DCN: Decorin; NS: Not Specified.

Biological experimentation to assess the behavior of in vitro cells differed from one study to another. The most frequently evaluated cell line was human gingival fibroblasts (hGFs) obtained from donors [9,10,12,16,17,19–21] or cell collections [8,11,15,18]. Three studies assessed the cell responses of epithelial cells (hGECs) [13,15,17]. Adhesion and proliferation were systematically assessed. Relative mRNA expression of adhesion-related genes or EMC components was also frequently investigated [8–10,13–15,17,18,20,21].

All the methodologies differed in terms of time points. For example, surface adhesion was evaluated in a range between 30 min [12,14,20,21] and 3 days [9]. Collagen production was assessed until day 7 [8], or until day 14 [18]. Controls also differed: rough titanium obtained after machining [19] or 3D printing [17] was used, as was polished titanium [18,20,21].

Table 4 summarizes the mechanical and biological results of the studies on the basis of the fabrication strategy employed. Three studies compared the fibroblast response on EA surfaces with unmodified Ti substrates [12,14,19]. Two articles included in their protocol a mechanical preparation of Ti surfaces before EA [9,16]. Nine studies evaluated hGFs behavior on EA surfaces followed by post-treatment. Regarding post-treatment, two studies out of nine proposed a simple post thermal treatment [8,10] whereas four performed a bioactive coating [11,13,15,17] and three studies proposed using NP and NT as a reservoir to deposit growth factors [18,20,21].

Table 4. Summary of the results of the studies reviewed on the basis of fabrication strategy. It was decided to keep the original names of the different groups in order to conform to the abbreviations chosen by the authors of the studies selected.

Surface Characterization of EA Surfaces				Biological Evaluation	
Study/ Year	**Surface Roughness of Tested Specimen and Control Surface**	**Morphology of the TNT/TNP (Diameter, Length, Tube Walls)**	**Water Contact Angle (WCA)**	**Evaluated Functions and Duration of Treatment**	**Results Compared to the Titanium Control Surface**
Electrochemical anodization + heat treatment					
Wang et al., 2020	Air-TNT: Ra = 45.8 ± 6.3 nm H2-TNTs: Ra = 51.4 ± 2.3 nm Control: Ra = 8.9 ± 2.4 nm	TNT Diameter: 100 nm Length: 1 µm	Air-TNT: 36.6 ± 2.0° H2-TNTs: 3.5 ± 0.8° Control: 95.1 ± 1.5°	Cell adhesion at 1, 2, and 4 h	Proliferation was higher on Air-TNT and H2-TNT surfaces at 7 d.
				Cell proliferation at 1, 3, 5, and 7 d	Cell adhesion on H2-TNT was higher than that of other groups.
				Cell morphology at 1, 4, and 24 h	More filopodia at 1 h and more elongated morphology at 4 h.
				Evaluation of focal adhesion at 4 and 24 h	Presence of mature elongated FA formed at the periphery of the cells on TNT surfaces.
				Migration at 12 and 24 h	Cells gradually filled the wound within 24 h.
				Gene expression at 4 and 24 h	At 4 and 24 h, HGFs on H2-TNTs showed higher mRNA expression levels of focal adhesion kinase and integrin-β1.
				Collagen production at 1, 4, and 7 d	At 1 h, 4, and 7 d, the collagen secretion from the HGFs on the H2-TNTs was higher than that on the air-TNTs and Ti control.
Xu et al., 2020	NS (Diagram without associated values) NT surface: 500 nm < Sa < 1 µm Control Ti surface: Sa ≈ 1.5 µm	TNT NT10: Diameter: 30 nm NT30: 100 nm NT60: 200 nm	NS (Diagram without associated values) WCA for NT surface < 40°. Hydrophilicity increased with the diameter. WCA for Ti Control surface ≈ 50°	Cell adhesion after 2 h	Cell adhesion was improved on NT10 and NT30 after 2 h but severely inhibited on NT60.
				Cell proliferation at 1, 3 and 7 d	NT10 and NT30 promoted cell proliferation, but NT60 decreased it.
				Cell morphology at 2 d	Cells on T10 and NT30 elongated further, and a large number of prominent filopodia and lamellipodia extensions was observed.
				Gene expression at 7 d	The expression of VCL and FN genes became increasingly higher for NT30 at NT10 at 7 d.

Table 4. *Cont.*

Surface Characterization of EA Surfaces				Biological Evaluation	
Study/ Year	**Surface Roughness of Tested Specimen and Control Surface**	**Morphology of the TNT/TNP (Diameter, Length, Tube Walls)**	**Water Contact Angle (WCA)**	**Evaluated Functions and Duration of Treatment**	**Results Compared to the Titanium Control Surface**
Mechanically prepared + Electrochemical anodization					
Gulati et al., 2020	TNP-60: Ra = 134.43 ± 33.8 nm Micro-Ti: Ra = 40.80 ± 3.2 nm Rought-Ti (Control): Ra = 74.57 ± 2.7 nm	TNP TNP-40: Diameter: 50 nm TNP-60V: Diameter: 60 nm TNP-80V: Diameter: 75 nm	NTP-40: 46.08 ± 0.68° NTP-60: 59.08 ± 1.36° NTP-80: 38.05 ± 0.64° Micro-Ti: 47.98 ± 2.02° Rought-Ti: 44.70 ± 0.28°	Cell adhesion at 1 h, 6 h, 1, and 3 d	After 6 h of seeding, cell length and cellular area were higher for TNP-40 and TNP-60 as compared to Rough and Micro-Ti.
				Cell viability at 1, 3, and 7 d	By day 7, Micro-Ti and NP surfaces enhanced cell proliferation.
				Cell morphology 1 h to 7 d	Even at 1 h, there were more filopodia on the NP surfaces. Fibroblasts formed close contact with the NP at all points.hGFs spread and elongate parallel to TNPs at 1 d.
				Gene expression at 1,3 and 7 d	Enhanced collagen I/III and integrin-β1 mRNA expression at day 3–7.
Gulati et al., 2018	TNS-50: Ra = 134.43 ± 33.8 nm TNS-70: Ra = 91.24 ± 7.1 nm Miro-Ti: Ra = 40.80 ± 3 nm	TNP TNS-50: Diameter: 50 nm Length: 8 μm TNS-70: Diameter: 70 nm Length: 12 μm	NS	Cell morphology at 1,6 h, 1, and 4 d	hGFs were elongated and confluent on the TNS surfaces and found to be aligned in the direction of the NP.
				Cell proliferation at 1, 4, and 7 d	No difference.
Electrochemical anodization only					
Llopis-Grimalt MA et al., 2019	NP: Ra = 31.3 ±1.9 nm Sku = 3.74 ± 0.39 nm Ssk = 0.2 ± 0.07 nm NN: Ra = 55.8 ±1.6 nm Sku = 2.81 ± 0.13 nm Ssk = 0.07 ± 0.04 nm Ti-Control: Ra = 28.9 ± 0.7 nm Sku = 6.78 ± 2.96 nm Ssk = 0.34 ± 0.24 nm	TNP NP: Diameter: 52.9 ± 0.9 Length: NS NN: Diameter: 77.7 ± 0.7 nm Length: 47.4 ± 0.5 nm	NP: 17.7 ± 1.3° NN: 84.3 ± 3.8° Control: 71.7 ± 8.7°	Cell adhesion after 30 min	Both surfaces (NN and Control) showed similar results for cell adhesion.
				Cytotoxicity analysis at 48 h	No difference of hGFs cultured with conditioned media.
				Cell proliferation at 2, 7, and 14 d	Metabolic activity of hGFs was higher in culture on NN surfaces.
				Collagen quantification at 14 d	Collagen deposition of hGFs was higher on NN surfaces.
				Cell orientation	hGFs cultured on NN surfaces exhibited a high frequency of alignment.
Ferra-Canellas et al., 2018	NP-S: Ra = 54.7 ± 1.4 nm Surface area = 26.4 ± 0.5 μm^2 Rsa = 5.41 ± 0.21% NP-B: Ra = 41.6 ± 5.5 nm Surface area = 30.4 ± 0.4 μm^2 Rsa = 21.6 ± 1.6%Ti-control: Ra = 51.7 ± 5.71 nmSurface area = 26.4 ± 0.2 μm^2 Rsa = 5.68 ± 0.86%	TNP NP-S: Diameter: 48.2 ± 1.2 nm NP-B: Diameter: 74.0 ± 3.3 nm	NP-S: 79.6 ± 2.2° NP-B: 65.5 ± 5.8° Ti-control: 53.2 ± 2.5°	Cell adhesion at 30 min	Cell adhesion was increased by the NP-B surface compared to other surfaces.
				Cytotoxicity analysis at 48 h	All surfaces gave cytotoxicity values under the 30% limit established.
				Cell proliferation at 7 and 14 d	Difference between donors.
				Gene expression at 14 d	Difference between donors.
				Collagen quantification at 14 d	Higher collagen deposition cultured onto NP-B for both donors with statistical difference only for donor B.
Guida et al., 2013	Oxidized: Sa = 0.076 μm (0.061–0.097) Sdr = 10.5% (7.39–24.2) Turned (Control): Sa = 0.036 μm (0.02–0.69) Sdr = 0.799% (0.212–2.48)	"Nano-tubules" External diameter: 119 ± 22 nm Internal diameter: 50 ± 11 nm	NS	Cell adhesion at 6 h	Higher numbers of adhesive cells were evidenced on oxidized surfaces.
				Cell proliferation at 48 h and 7 d	The proliferation rate was higher on oxidized surfaces. The maximum difference was reached at 7 d.
				Cell morphology at 6 h	Many cellular processes were visible on oxidized surfaces. At higher magnification, intimate interactions between filopodia and the nano-tubular structures were observed. More evident spreading could be observed on the oxidized surfaces.
				Collagen synthesis 6 h, 48 h, 7 d	hGFs plated on oxidized surfaces showed to synthesize a higher amount of protein at 7 d.

Table 4. *Cont.*

Surface Characterization of EA Surfaces				Biological Evaluation	
Study/ Year	**Surface Roughness of Tested Specimen and Control Surface**	**Morphology of the TNT/TNP (Diameter, Length, Tube Walls)**	**Water Contact Angle (WCA)**	**Evaluated Functions and Duration of Treatment**	**Results Compared to the Titanium Control Surface**
Electrochemical anodization + Deposition/coating and biopolymer conjugation					
Zheng et al., 2020	NS	TNT Diameter: 100–170 nm Length: 1.2 μm	NS (Diagram without associated values)	Cell adhesion at 4 h and 24 h	At both times, Ti-O2-NT with Au decorations exhibited better affinity towards hGFs compared with NT or control surfaces.
				Cell proliferation at 1, 3, 5, and 7 d	Higher proliferation on NT-Au surfaces compared with NT or control surface at all time points.
				Migration at 24 h	Improvement in wound contraction observed on NT-Au surfaces compared to control group.
				Gene expression at 24 h	AU-NT surfaces upregulated the gene expression level of FN and FAK.
				Phosphorylated-FAK and fibronectin expression at 24	Au-NT surfaces enhanced the protein expression of FN and pFAK.
Wang et al., 2019	NT-Ti: Sa = 22.1 ± 0.23 nm Chi/Col-Ti: Sa = 17.7 ± 0.12 nm Chi/Col/pLAMA3-CM-Ti Sa: Sa = 15.4 ± 0.17 nm S-Ti (Control): NS	TNT Diameter: 100 nm	S-Ti: 46.62 ± 4.66° NT-Ti: 12.86 ± 1.63° Chi/Col-Ti: 30.48 ± 1.84° Chi/Col/pLAMA3-CM-Ti: 29.12 ± 4.04°	Cell adhesion at 4 h	Adhesion was better on S-Ti than on NT-Ti Coated surfaces allowed better adhesion than S-Ti or NT-Ti.
				Cell morphology at 2, 6, 12 h, and 3 days	On NT surfaces and coated surfaces, hGECs were spherical, and filopodia extensions were observed after 2 and 6 h. On coated surfaces, at 12 h, cells were well-flattened with filopodia and lamellipodia.
				Cell viability 4 h, 1, 3, 5, and 7 d	No difference was found among the groups.
				Gene expression at 48 h	The LAMA3 and ITGβ4 expression levels were decreased in cells cultured on NT-Ti compared with those cultured on the control ones. Biological coating further increased the expression levels of both genes.
				Protein synthesis at 3 d	hGECs on the coated specimen presented relatively higher protein expression levels of proteins (LAMA3, ITGβ4).
Nojiri et al., 2019	NS	TNT Diameter: 67 nm	NS	Cell adhesion at 4 h	On NT surfaces without collagen, limited numbers of hGEC were seen compared with Col-NT surfaces.hGEC exhibited round-up morphology of weak adhesion.
Xu et al., 2018	AO (NT surface): Ra = 2.15 ± 0.04 μm AOC (NT + CaP): Ra = 2.15 ± 0.06 μm SLM (As built Ti): Ra = 7.57 ± 0.32 μm MP (Mechanically polished): Ra = 0.39 ± 0.01 μm	TNT Diameter: 70–90 nm Length: 200–250 nm	AO (NT surface): 40.7° AOC (NT + CaP): 18.3° SLM (rought Ti): 73.9° MP: 76.3°	Cell adhesion and cell morphology at 24 h	Protusions extending from the lamellipodia were visible on hGEC and wrapping around the NT. hGFs were more stretched and presented more extended lamellipodia.
				Cell proliferation by at 1,3,5, and 7 d	hGECs: AOC and MP surfaces > AO and SLM surfaces at 1,3,5, and 7 d. hGFs: AOC > AO > MP > SLM at 1,3,5, and 7 d.
				Gene expression at 7 d	hGEC: (AOC = MP) > (AO = SLM) at 7 d. hGFs: expression levels of FN and VCL followed the order of AOC > AO > SLM > MP. For ITGα3 and ITGβ1: AOC > AO > MP > SLM.

Table 4. *Cont.*

Surface Characterization of EA Surfaces				Biological Evaluation	
Study/ Year	**Surface Roughness of Tested Specimen and Control Surface**	**Morphology of the TNT/TNP (Diameter, Length, Tube Walls)**	**Water Contact Angle (WCA)**	**Evaluated Functions and Duration of Treatment**	**Results Compared to the Titanium Control Surface**
				hEGF protein secreted (for hGEC) and type I collagen synthesis (for hGF) at 1,2 and 4 d	hGEC: SLM and AO groups had lower expression than the MP and AOC groups after 7 d. hGFs: AOC > AO > MP > SLM at 7 d.
EA + Therapeutic delivery (loading)					
Liu et al., 2014	NS (Diagram without associated values) NT: Ra ≈ 200 nm NTB (Bovine serum albumin loading): Ra > 200 nm PT (Control): Ra < 200 nm	TNT Diameter: 80–100 nm Tube walls thick: 15–20 nm	NS (Diagram without associated values) PT > NT > NTB	Cell adhesion 1 and 3 h	At 1 h and 3 h: NTB > NT > PT.
				Cell proliferation at 3, 4, 7, and 14 d	No difference before 14 d. The proliferation activity of the hGFs increased over time on all surfaces.
				Cell morphology at 1, 3, 9, and 24 h	3 h after seeding, hGFs displayed ellipsoid spherical shapes with many pseudopodia anchoring to the TNT surfaces. At 9 h, they extended further. On the NTB surfaces, hGFs revealed many protruding pseudopodia at 1 h.
				Gene expression at 3, 4, 7, and 14 d	Gene expression on NT surfaces > PT surfaces after 4, 7, and 14 d. Gene expression on NTB surfaces > on PT surfaces after 7 and 14 d. Gene expression on NTB surfaces < NT surfaces after 3, 4, 7 d.
				Collagen synthesis at 3, 4, 7, and 14 d	COL-1 concentrations on PT surfaces > NT surfaces at 3 and 4 d. NT surfaces > PT at 7 d. The COL-1 concentration was the lowest on the NTB surfaces after 3, 4, and 14 d.
Ma et al., 2012	NT: Ra = 4.96 ± 0.5 nm NT-F-L/M/H (FGF2-immobilized at different concentrations): Ra = from 7.25 ± 0.97 nm to 9.42 ± 1.99 nm PT: Ra = 32.6 ± 3.45 nm	TNT Diameter: ≈100 nm Length: 588.8 ± 31.92 nm	NS	Cell adhesion at 30, 60, and 120 min	The number of adhering cells on NT-F-L and M was higher than those on the PT, NT, or NT-F-H at all times points. NT-F-M showed the highest cell adhesion Cell adhesion on NT surfaces was decreased compared with PT.
				Cell proliferation at 1, 3, 6, and 9 d	NT surfaces enhanced proliferation at 3 d compared with NT surfaces. NT-F-L and NT-F-M enhanced proliferation compared with PT surfaces at all time points.
				Cell morphology at 3 d	Observed differences were slight.
				Gene expression at 3, 6, and 9 d	NT-F-L and NT-F-M showed beneficial ECM-related gene expression.
Ma et al., 2011	NT: Ra = 27.76 nm RZ = 260.5 nm NT-Ag (Silver-loaded): Ra = 29.10 nm RZ = 128.1 nm NT-Ag-F (Siler/FGF2 immobilized): Ra = 34.18 nm RZ = 156.2 nm PT: Ra = 58.1 nm RZ = 128.5 nm	TNT Diameter: ≈ 100–120 nm	NS (Diagram without associated values) (PT and NT-Ag-F) > (NT and NT-Ag)	Cytotoxicity analysis at 24, 48, and 72 h	No difference in cellular response.
				Cell adhesion at 30, 60, 120 min	Cell adhesion was higher on NT-Ag-F surfaces than those on PT, NT, and NT-Ag at all time intervals. NT surfaces seemed to inhibit cell adhesion.
				Cell proliferation	Cell proliferation was better on NT-Ag-F surfaces than on PT, NT, and NT-Ag at all time intervals.
				Gene expression	HGFs cultured on NT-Ag-F surfaces showed advantageous gene expression.

Abbreviations: TNT: titania nanotubes; TNP: titania nanopores; EA: electrochemically anodized; MP: Mechanically polished; FA: focal adhesion; Ra: average roughness; Ssk: surface skewness; Sku: surface kurtosis; AO: anodic oxidation; SLM: selective laser melting.

3.4. Nano Surface Characteristics of Anodized Titanium

3.4.1. Morphological Characteristics and Surface Roughness

The fabrication of nanoporous structures like nanopores (NP) or nanotubes (NP) by EA modifies surface topography. In the included studies, Ra, which is the arithmetical mean deviation of the profile assessed, is the most widely used one-dimensional roughness parameter. After electrochemical anodization, the reported Ra varied on average from 4.96 nm [20] to 2 µm [17]. This variation was due to the initial surface condition of the selected Ti surfaces, which varied for each study. Some surfaces were polished mechanically, while others were left in a rough state, either after machining or 3D printing. The highest surface roughness was found for a titanium material obtained by an additive process that initially increased the surface roughness [17] due to powder particle agglomeration. The lowest roughness was described for a titanium material polished mechanically before EA [20]. Most of the studies reported that anodized Ti surfaces obtained from a polished or machined titanium surface exhibited Ra values measured by AFM in the range of 40 to 80 nm. The average values reported by the studies were 45.8 nm [8], 40.8 nm [9], 55.8 nm [12], 54.7–41.6 nm [14], and 76 nm [19]. Such reported values were lower than 0.2 µm which can be considered a threshold below which no further significant changes in bacterial adhesion might be observed [25].

Since Ra does not distinguish between hollows and protrusions, this parameter might be insufficient for the description of the nanoarchitecture of surfaces, and misinterpretations about the roughness can be made. For instance, a study showed that the Ra was 2 times lower for anodized surfaces than for polished surfaces (27.76 nm vs. 58.17 nm) while Rz (which is the average value of the absolute values of the heights of the 5 highest-profile peaks and the depths of the 5 deepest alleys within the evaluation length) was 2 times higher for anodized surfaces (260.5 nm vs. 128.5 nm) [21]. The surfaces of the anodized surfaces may appear smoother than before anodizing, but it should be recalled that the pores or tubes generate a depression whose depth affects roughness. Thus, some studies proposed to analyze the surface topography through additional parameters. Guida et al., 2013 [19] did not consider Ra but Sa, which is the extension of the Ra parameter to a surface. Furthermore, they correlated the Sa measurement to the interfacial area ratio developed (Sdr). Sdr is expressed as the percentage of additional surface area due to the texture as compared to an ideal projected plane for which Sdr = 0. They reported that anodized surfaces show a surface area 10% larger than the projected surface compared to 1% on the polished surface. Similarly, Ferra-Canellas et al., 2018 [14] indicated that the surface area difference (Rsa), defined as the percentage increase of the 3D surface area over the projected 2-dimensional surface area, was 4 times higher for NP-B anodized surfaces than for control surfaces despite smaller Ra values for anodized samples.

From the 3-dimensional viewpoint, anodized surfaces offer quantitatively more reactive sites than "flat" surfaces. This "additional" surface is indeed provided by the internal walls of the NT or NP. This particularity would enhance the adhesion of the cells since it emphasizes the possibility of anchoring sites. From the 2-dimensional viewpoint, the presence of NT quantitatively decreases the surface area due to the hollow structure.

It should be noted that the values found in these studies are dependent on the experimental limitations inherent to the technology used and the surface geometry. For instance, the pyramidal shape of the AFM tip probably prevents it from entering into the bottom of the NT/NP.

The nanotopography is dependent on the morphology of NT/NP, whether it is the diameter (pore size), length (or depth), thickness of the walls, or inter-gap distance in the case of NT, or the inter-pore distance in the case of NP.

In the included studies, the internal diameters varied from 30 nm to 200 nm [10]. These values generally correspond to a measurement made along the longest axis of the pores, since NPs and/or NTs never exhibit perfect circularity. Studies with a high voltage anodizing process show larger pore sizes [9,10,15,16]. This is in line with literature data showing that the diameter of the TiO_2 NT/NP increases linearly when increasing

anodizing voltage. Regarding NT diameter, most studies report values between 90 and 120 nm, whether for a potential of 50 V for 15 min [8], 30 V for 3 h [10], 20 V for 30 min [13], 20 V for 45 min [17], 25 V for 1 h [18], 20 V for 24 h [19], and 20 V for 45 min [20,21].

Other morphological characteristics such as length or wall thickness were not systematically reported in these studies. Interestingly, Wang et al., 2020 [8] analyzed the longest NTs with a length of about 1000 nm for a high voltage (50 V) associated with a short time (15 min) in a viscous electrolyte. Xu et al., 2018 [17] reported lengths ranging from 200–250 nm, and Ma et al., 2012 [20] described NTs with lengths of 588.8 ± 31.92 nm. These "shorter" NTs were found mainly for purely aqueous electrolytes, which was also in agreement with previous reports [4]. Only one study reported a value for wall thickness equal to 15–20 nm [18]. In another study, by calculating the difference between the reported external diameter and the internal diameter, the deduced wall thickness of the "nano-tubules" was about 70 nm [19]. This wall thickness is a very important criterion since it provides an anchor point for the cytoplasmic extensions of the gingival cells in the case of NT. Furthermore, the wall thickness also influences the chemical nature of the reactive sites. In the case of NP, it is the distance between the pores that is important [9].

The different post-functionalizations of anodized surfaces also change the roughness. Ma et al., 2011 [21] showed that surfaces functionalized with silver nanoparticles and FGF (fibroblast growth factors) have a higher surface roughness than simply anodized surfaces (34.18 nm vs. 27.76 nm). Similarly, Liu et al., 2018 [18] showed that the surface roughness on bovine serum albumin-functionalized surfaces has higher Ra values (up to 700 nm) than anodized surfaces (200 nm). On the other hand, the surfaces modified by a coating based on chitosan and collagen tended to smooth the surface since they showed a lower Sa value (17.7 nm) than the simply anodized surfaces (22.1 nm) [13]. These remarks suggest that the post-functionalization grafted entities do not adsorb on the same adhesion sites of the nano-structured surface. For example, when the Sa is lower, it would imply that the biomolecules such as biopolymer could be located in the "hollows" of the surface, thus reducing the roughness.

To summarize, anodizing modifies the roughness at the nanometric scale. This nanometric modification does not affect the roughness at the micron scale, which is dependent on the initial surface condition of the material.

3.4.2. Morphological Characteristics and Surface Roughness

- Wettability

Electrochemical anodization improves wettability in the case of NT formation. Water contact angle (WCA) is systematically decreased for anodized surfaces with the presence of NT compared to a non-anodized control surface [8,10,11,13,17,18,21]. It seems that the morphological characteristics of the NT and, more specifically, the diameter, influence wettability: the larger the diameter, the smaller the contact angle [10]. NP features lead to a less hydrophilic surface than NT [9,12] even if a pore size above 70 nm may allow a better WCA than a pore size of 50 nm [9,14].

All the included studies show that WCA on anodized surfaces was less than 90°, which implies that all the anodized surfaces, no matter NP or NT morphology, can be considered as hydrophilic. This hydrophilic behavior associated with a nanostructure surface could induce the deposition of adhesion-related proteins from physiological fluids in the NT/NP.

Wettability is directly related to surface energy. Ma et al., 2011 [21] showed that the higher the contact angle, the lower the surface energy calculated by the Owens equation [21]. Surface energy modulates the ability of the surface to establish electrostatic, Van der Waals, or hydrogen bonds with a polar medium, like water, and then plays a big role in the initial adsorption of protein and cell adhesion.

Functionalization also changes wettability. Wang et al., 2020 reported that surfaces anodized and then modified with a coating of collagen and chitosan have a significantly higher contact angle than simply anodized surfaces [13]. Conversely, surfaces anodized

then coated with calcium phosphate nanoparticles [17], surfaces anodized and then loaded with bovine serum albumin (BSA) [18], and surfaces decorated with gold nanoparticles [11] are more hydrophilic than anodized surfaces alone.

- Crystalline phase

The crystalline or amorphous nature of TiO_2 is also one of the parameters affected by the anodization treatment, and especially by the possible post-anodization heat treatments. Two studies assessed the absence of crystallinity of the oxide layer in the case of NT formation [8,10]: after anodization, TiO_2 NTs are generally in amorphous form. The authors performed post thermal treatments to modify the crystallinity of the oxide layer of the anodized parts. After annealing in air at 450 °C for 2 h, the XRD (X-ray diffraction) patterns showed Ti and anatase peaks without any rutile or amorphous peaks [10]. Similarly, after annealing in air at 550 °C for 2 h, or at 500 °C for 4 h in air with a controlled hydrogen atmosphere, the XRD pattern showed that the amorphous titanium changed to an anatase phase [8]. This annealing resulted in an increase of the compact layer at the metal/NT interface, which led to a decrease in NT length. Above a certain temperature, the tubular structure is lost. The conversion from amorphous to anatase phase can have consequences on mechanical, chemical, electronic, optical, and biomedical properties since the anatase crystal type possesses good anti-bacterial properties. Although none of the included studies mentioned this point, it should be noted that raising the annealing temperature to 580 °C may remove surface hydroxyl groups and even cause the NP/NT structure to collapse [26], thus reducing the other properties (i.e., hydrophobicity) [27].

3.5. Biological Results of the Studies Reviewed

3.5.1. Biological Behavior of Human Gingival Fibroblasts (hGFs) Regarding Anodized Surfaces

- Cell adhesion

The majority of the studies presented in this review showed that a titanium surface modified by anodization allows, in vitro, better adhesion of hGFs on the surface compared to conventionally polished or machined titanium.

Based on measures performed on SEM images, Gulati et al., 2020 [9] showed that hGFs seeded on nanoporous surfaces superimposed on micro-scale features exhibited a more elongated and spread-out shape at 6 h than hGFs seeded on control surfaces (rough or polished). After DAPI staining and analysis by fluorescence intensity at 1 and 3 h, Liu et al., 2014 [18] showed that cell adhesion at 1 and 3 h was better on NT surfaces (with an Ra equal to 200 nm, a diameter of 100 nm, and a wall thickness of 15–20 nm) than on polished surfaces. Using colorimetric tests, Ferra-Canellas et al., 2018 [14] reported that at 30 min, hGFs statistically adhered better on nanoporous anodized surfaces (with a pore size equal to 74.0 $\pm$ 3.3 nm and an Rsa 4 times higher than the control surface). Similarly, Guida et al., 2013 [19] proved that at 6 h, adhesion is statistically increased when hGFs are in contact with nano-tubular anodized surfaces (with a diameter of 120 nm and thick walls of 70 nm) compared to the titanium control surface.

In contrast, other studies did not report favorable results. Llopis-Grimalt et al., 2019 [12] concluded that at 30 min, there are no differences regarding HGFs adhesion between control and nanoporous anodized (NN) surfaces. These NN surfaces with a pore size equal to 77.7 $\pm$ 0.7 nm present a lower wettability than the control surface. Ma et al., 2012 [20] reported that NT surfaces with a diameter of 100 nm and without functionalization significantly decreased cell adhesion at 30 min, 1 h, and 2 h. The authors explained that nano-tubular anodized surfaces present "hollows" that quantitatively decrease the contact area available for cell adhesion. This study did not report the value of wall thickness, but it was possible through SEM images to provide a rough estimation of about 10 nm. However, it has been described that filopodia (which are thin cytoplasmic extensions in the region of tens of nanometers) can detect surface topographic features of about 15 nm [28], as presented in Liu et al., 2014 [18]. The main difference between Liu et al., 2014 and Ma et al., 2014 resided in the composition of the electrolyte. In one study [20], the aqueous

electrolyte led to the formation of NT arrays with thin wall thicknesses, while in the other, the viscous glycerol-based electrolyte with only 15% water content [18] led to an NT with greater wall thickness, which is consistent with a previous study [29]. Although ultrathin walls are essential for some applications (such as photocleavage of water), favoring a wall with at least 15–20 nm thickness would be interesting for biomedical applications.

These quantitative findings regarding adhesion are consistent with qualitative analysis since all the studies investigating hGFs morphology through SEM images or by immunofluorescence agreed that hGFs in contact with an EA surface present a morphology favorable to adhesion in contrast to similar cells cultured on control Ti surfaces. All the authors observed the presence of more lamellipodia and filopodia than on a polished or machined control surface [9,16–20].

At a higher magnification on NT surfaces, filopodia anchor on the edges of the tubes (and not inside the tube), which occurs at a very early point [8,10]. On NP surfaces, the authors described an intimately close correlation of fibroblast projections with the nanopores [9]. Figure 5 shows the morphology of hGFs spreading on TiO_2 NP at day 1 of the culture.

Furthermore, when nanopores are aligned with micro-machining lines fabricating EA, hGFs stretch along the direction of nanopores. This better alignment of the cells is interesting because the secreted proteins, like collagen, could be deposited and oriented in the same direction and not randomly [30].

In addition, some of the studies found in this work also highlight the possibility that anodized surfaces promote not only better adhesion, but also faster attachment of gingival fibroblasts [9,18]. This kinetic aspect is crucial as it is known that during the insertion of a biomaterial, there is "a race to the surface" between epithelial cells, fibroblastic cells, and bacterial cells [31,32]. If local human cells colonize the surface promptly and create a close loop of connective tissue around the oral implant, it may prevent bacterial invasion.

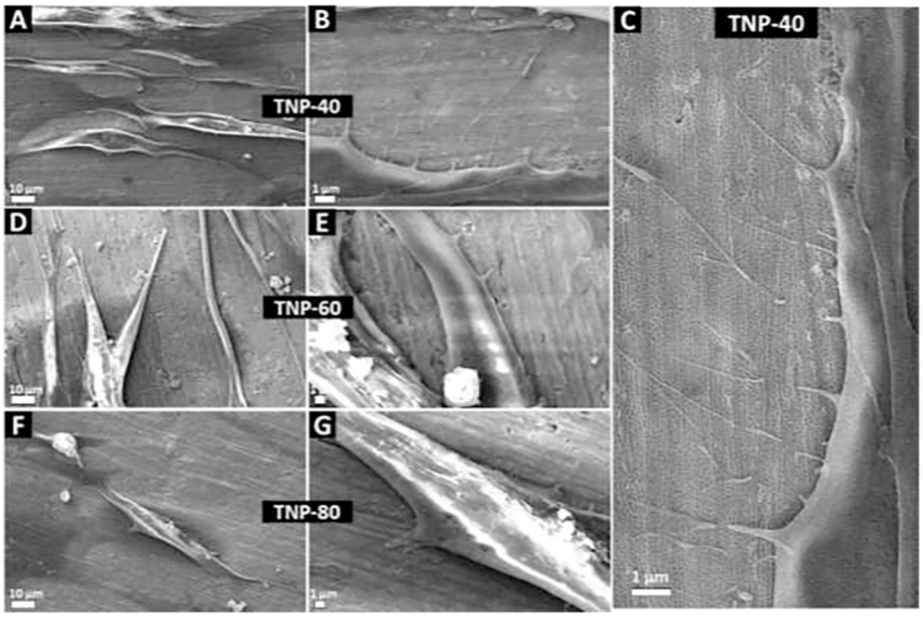

Figure 5. hGFs on TiO_2 surface with NP after 1 day, (**A**–**C**) TNP-40, (**D**,**E**) TNP-60, (**F**,**G**) TNP-80. Adapted with the permission from [5180781375259] [9].

This adhesion is dependent on the adsorption of proteins. Since the size of plasma proteins such as fibronectin is nanometric, the adsorption kinetics of these proteins, as well as the quantity adsorbed, are influenced by surface properties at a very small scale. These surface properties are based on the nature (chemistry and structure) of the reactive sites located on the surface and especially on the tube edges in the case of NT. These characteristics are closely related to several physical parameters such as roughness, surface

energy, surface charge (isoelectric point), and wettability. Since anodizing changes all these surface properties, this process has a significant influence on adsorption. Overall, it appears that anodized surfaces provide better protein adsorption. However, this assertion is true up to a certain limit. Indeed, beyond a diameter of about 70–100 nm [10], proteins are no longer adsorbed on the surface of the NT but probably tend to migrate to the bottom of the wells inaccessible to cells [8]. Furthermore, protein adhesion to the surface of the transgingival component depends on the spatial distribution of surface charges relative to the distribution of plasma protein charges. To avoid protein unfolding leading to denaturation, a certain level of hydrophilicity should not be exceeded. An excessive surface energy of anodized surfaces could explain why cells adhere less well on anodized surfaces than on control surfaces [21].

Depending on the pressures and mechanical stimuli that the cells perceive through their adhesion to the substrate and also through the intercellular contacts that are formed, a series of intracellular biochemical reactions will be triggered. These reactions will influence cell proliferation, the secretion of ECM components, and even promote cell migration, thus influencing wound healing.

- Cell proliferation

Most of the studies analyzed report that, compared to conventionally used smooth surfaces (polished or machined), EA surfaces ensure better fibroblast proliferation. Proliferation is analyzed through metabolic activity by several tests based on the incubation of colorimetric markers at different times. For Guida et al., 2013 [19], the metabolic activity of hGFs in contact with nano-tubular EA surfaces was slightly better at day 2 and then much higher at day 7, whereas for Gulati et al., 2020 [9], the metabolic activity of hGFs in contact with EA surfaces was increased compared to control raw surfaces only at day 7. In addition, there were no significant differences between the 40 V, 60 V, and 80 V anodized surfaces with nanopore diameters of 50 nm, 60 nm, and 75 nm, respectively. Llopis-Grimalt et al., 2019 [12] also tended to find an improvement in metabolic activity at day 14, i.e., at the end of the experiment. They did not find any difference at day 2 or day 7 between hGFs seeded in contact with polished surfaces or in contact with nanoporous surfaces with a diameter of about 80 nm. Liu et al., 2014 [18] followed this trend as enhanced hGFs metabolic activity on surfaces with an NT diameter of 80–100 nm compared to polished surfaces was detectable only at day 14. These observations are consistent with the "normal" in vivo biological processes that take place after any injury. Within the first 2 days, processes related to inflammation appear, then after this 48 h period, new tissue formation occurs, characterized by cell proliferation. Finally, after 10 to 15 days, tissue remodeling processes are in place.

Conversely, Ma et al., 2012 [20] and Ma et al., 2011 [21] showed a slight increase in metabolic activity at day 3 that was not found at day 6 or day 9. This was in line with the results they described regarding adhesion and correlated with NT morphology in the previous paragraph. On the other hand, Xu et al., 2018 highlighted better metabolic activity for hGFs on anodized surfaces compared to those grown on polished surfaces at all time points (1st, 3rd, 5th, and 7th day). The difference with previous studies resided in the fact that Xu et al., 2018 anodized titanium surfaces obtained by the SLM additive manufacturing technique. The anodized surfaces exhibited not only nano roughness due to the presence of NT but also microroughness inherent to the manufacturing process, possibly explaining the better cell proliferation in vitro at the first time point.

- Influence on the expression of soft tissue integration genes and production of specific proteins by hGFs

The majority of studies included in their protocol analysis by RT-qPCR (Reverse Transcriptase Polymerase Chain Reaction) of the expression of genes coding either for proteins found in cell adhesion mechanisms (such as fibronectin, vinculin, laminins, or integrins) or for the production of structural proteins of the extracellular matrix (such as

collagen I and III). Two studies also observed markers that can contribute to angiogenesis, such as VEGF (vascular endothelial growth factor) [9,20].

Regarding the relative gene expression level of adhesion-related proteins, Gulati et al., 2020 [9] showed that the expression of integrinβ1 (important receptors mediating cellular binding onto the implant surface) is increased for hGFs seeded on anodized surfaces with 60 and 75 nm diameter NP compared to control surfaces at day 7. According to Xu et al., 2018 [17], hGF grown in contact with EA surfaces express FN and VCL genes encoding fibronectin (an important adhesion protein) and vinculin (an important cytoskeleton bonding protein associated with adhesion strength and migration) better at day 7 than hGF in contact with polished surfaces. Better gene expression related to adhesion is, most of the time, correlated to a better cell attachment. However, an overexpression of these genes may be related to reverse compensation. Ma et al., 2012 [20] showed better expression of ITGB at days 3, 6, and 9 on surfaces with NT than on polished surfaces, which was in contradiction with the results related to adhesion and proliferation. They concluded that the cells compensated for their lack of adhesion by expressing more mRNA (messenger ribonucleic acid) coding for β-integrin. Thus, it was preferable to complete the measurement of gene expression either by qualitative or quantitative analyses to ensure that the cell was correctly fulfilling its functions.

Gulati et al., 2020 [9] showed that hGFs in contact with 60 nm and 75 nm diameter nanoporous EA surfaces expressed the angiogenesis-associated marker VEGF better at day 7 than hGFs grown in contact with control surfaces or in contact with surfaces with 50 nm diameter NP. Ma et al., 2012 [20] showed that hGFs in contact with anodized surfaces expressed VEGF significantly better than polished surfaces. However, they added that an overexpression of this growth factor might reflect the persistence of inflammatory mechanisms or edema unfavorable to healing.

Collagen is the major component of extracellular matrices in gingival connective tissue and especially COL-1. The correct gene expression and production of COL-1 and/or COL-3 suggests that the surface on which the cells are cultured optimizes their capacity to secrete components essential for the adhesion, healing, and maintenance of homeostasis. All the studies that evaluated COL-1 and/or COL-3 mRNA expression and collagen secretion agreed that hGF cultured on anodized surfaces gave better results than hGFs seeded on conventional Ti substrates [8,12,14,17–19]. EA surfaces could favorably influence hGFs' function. Despite the enhanced production of collagen fibers, the latter was not necessarily arranged in a favorable manner relative to the surface. Ideally, the optimal surface would stimulate a perpendicular fiber arrangement to mimic the anatomy of the peri-implant tissue in front of a natural tooth. It is very difficult to recreate this in vitro condition, and one of the studies included established an electrophoretic method for the perpendicular implantation of collagen into TNT15. They showed an overhead view of NT surfaces COL-1 as nanodots indicating the perpendicular attachment.

3.5.2. Biological Behavior of Human Gingival Epithelial Cells (hGECs) to Anodized Surfaces

The three studies that investigated the behavior of hGECs on NT surfaces reported similarly negative results. Wang and al. 2020 showed on fluorescence images that NT surfaces decreased the number of attached cells after 4 h compared to the control surface [13]. After 48 h of culturing hGECs in contact with an NT surface (100 nm diameter) without functionalization, the LAMA3 and ITGB4 expression levels (which are the major components of hemidesmosome and basement membrane) were decreased compared with those cultured on the control surface. In a consistent way, SEM observations displayed that hGECs present an elongated irregular shape instead of a spherical one with very few filopodia. Interestingly, Xu et al., 2018 [17] described a morphological shape favorable to adhesion with lamellipodia anchoring on the EA surfaces, but gene expression relating to adhesion after 7 days was lower on NT surfaces than on polished control, as was cell proliferation. Nojiri et al., 2019 indicated that on NT surfaces without collagen grafting, hGECs exhibited round-up morphology signifying weak adhesion [15].

3.5.3. Multi-Functional Surfaces

In order to amplify the bioactivity of nano-tubular surfaces and simultaneously boost anti-bacterial activity, some authors have proposed different surface functionalizations. Two main modifications may be considered, whether by the chemical reactivity of the surface via the reactive sites (H+, OH) (Figure 6a) or by the shape of the NT/NP that acts as a reservoir (Figure 6b). Thus, the authors filled the NP/NT with growth factors or anti-bacterial agents, or performed biological coatings/depositing by grafting peptides, proteins, or nanoparticles. Sometimes, both these modifications were performed [21].

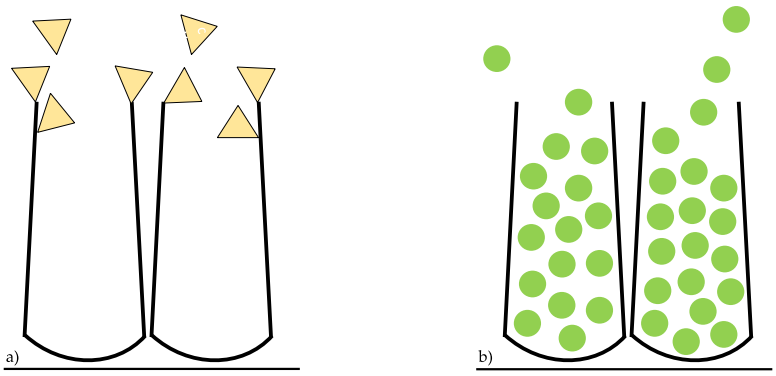

Figure 6. Various therapeutic and bioactivity enhancements performed on nanotubes. Adapted from Guo T et al., 2021. (**a**) illustrates how the reactive site on the surface may be used to graft different coatings (like nanoparticles or biopolymer); (**b**) illustrates how different substances may be incorporated into NT (as a growth factor, nanoparticles, anti-bacterial drugs) in order to ensure progressive delivery.

- Therapeutic delivery

Thanks to the hollow-core structure, NT and Np may be used as reservoirs by loading different agents. Liu et al., 2014 [18] reported that a BSA (bovine serum albumin) coating positively affects early-stage adhesion, enhances cell spreading, and promotes COL-1 expression of hGFs even if BSA coating suppresses COL-1 secretion at all-time points compared to NT surfaces and polished control. Ma et al., 2012 [20] functionalized their EA surfaces, whose NT were about 500 nm long, with fibroblast growth factors (FGF) which are proteins that activate cell multiplication and function. They showed that hGFs adhesion is better on functionalized surfaces than on simply anodized surfaces. On the other hand, surfaces functionalized with FGF were favorable for the adhesion and proliferation of hGF only at an optimum concentration. Above this concentration (500 ng/mL), the functionalization became detrimental for adhesion. The authors added that the release of the substances loaded was inevitable and that the effect did not continue over time. The length and the diameter of the NT regulated release behavior over time.

- Polymers/biomolecule/nanoparticles conjugation and coating

Synthetic or natural biopolymers and nanoparticles can be grafted using the reactivity of the surface hydroxyl groups located on the NT arrays.

As a natural biopolymer, a chitosan/collagen coating containing a plasmid pLAMA3-CM encoding a motif of the C-terminal globular domain of LAMA3 (which is associated with the formation of hemidesmosomes HD) was proposed to modify EA surfaces with NT [13]. Following 48 h of culture, hGECs cultured on functionalized NT surfaces effectively took up the incorporated plasmids, resulting in better attachment and the formation of HD compared to simply NT surfaces.

Similarly, another study [15] attached collagen protrusion on NT surfaces using different methods and analyzed the bonding stability of the collagen after sonication cycles by

FTIR-ATR. They reported that a stable bond was achieved between the EA surfaces and collagen despite drastic ultrasonication.

Xu et al., 2018 [17] modified EA surfaces with calcium phosphate (CaP) coating. They showed that hGECs and hGFs adhesion and proliferation were better on NT surfaces coated with CaP compared with simply NT surfaces.

In order to develop a surface with antimicrobial properties, Ma et al., 2011 [21] immobilized Ag nanoparticles associated with a growth factor (FGF-2) coating. They show that the adherence ratio of hGFs and proliferation was higher than those on the polished or simply NT surfaces. The immobilization of FGF-2 can offer various cell-substrate contact areas and reverse the negative effect due to the NT array. This surface can upregulate type I collagen expression and ITGB at days 3 and 6 compared to polished or NT surfaces. They concluded that this modified surface has potential use in dental implant abutment. Another study [11] developed a novel implant surface of TiO_2 decorated with gold nanoparticles (Au) due to their anti-bacterial properties. Indeed, the adjunction of Au particles enhanced the photocatalytic potential of TNT upon visible-light irradiation. They reported that Au nanoparticles were absorbed onto the tube wall located deep inside the tubular structure. This incorporation of Au on NT surfaces greatly improved hGF response as adhesion, migration, and proliferation.

- Crystalline structure

After EA, Wang et al., 2020 [8] annealed the Ti specimen under specific hydrogen conditions in order to obtain hydrophilic surfaces. They showed that these modified surfaces enhanced the adhesion of hGFs rapidly and improved the relative gene expression level and ECM synthesis of the hGFs. Interestingly, they performed a wound-healing assay to study the effect of the EA surfaces on hGF migration. They concluded that cells on EA surfaces modified by a thermal hydrogenation technique show a faster migration speed than those on the control Ti surfaces. They also observed after immunofluorescence staining that cell morphology and cytoskeletal actin filaments are better organized when hGFs are cultured on EA and treated surfaces compared to control.

To sum up, because all the included studies exhibited a positive influence after functionalization, such as biological coating, the incorporation of anti-bacterial agents, or heat treatment, the modification of EA Ti surfaces seems to be the key for taking full advantage of the process.

4. Conclusions

Within the limitations of this systematic review based on in vitro studies, it can be safely speculated that EA Ti surfaces influence the bioactivity of the compound. The modified EA surfaces improve hGFs response and thus probably positively influence connective tissue regeneration compared to traditional polished or machined Ti surfaces, but negatively influence hGECs behavior. Regarding hGFs, this positive influence in terms of adhesion, proliferation, and functions is only true if the surface's characteristics such as morphology, roughness, chemistry, and energy are optimal at the nanoscale. Even though it remains difficult to identify an optimal morphology for enhanced cell behavior, it can be assumed that the pore diameter, as well as the wall thickness, are the key factors. An ideal pore size seems to be situated between 70 and 120 nm. Above a certain diameter, hydrophilicity is a disadvantage for the bioactivity of hGFs. In the case of NT, the wall thickness must be at least 15 nm to anchor the cytoplasmic extensions. In the case of NP, the thickness between the walls prevails. A nano-tubular morphology is favorable for depositing anti-bacterial agents or growth factors into the length of the tube. However, it has been reported that the NP structure is more mechanically stable than NT. It is difficult to conclude on the optimum crystallinity of the oxide layer to promote the bioactivity of hGFs even if it seems that an anatase form is preferable.

To achieve this ideal ordered NT or NP surface and ensure the best performance, anodization conditions such as voltage, time, electrolyte (nature, composition, viscosity, age, acidity), and temperature must be optimized. Associating NT or NP with other

modifications may be considered systematically. Indeed, all the studies, including a preliminary preparation of the Ti surface before anodization as well as a post-modification such as functionalization, showed better biological results for anodized and functionalized surfaces than for anodized surfaces alone. EA surfaces associated with a biological coating positively influence both hGFs and hGECs behavior and thus may improve the biological phenomena that can occur between surfaces and the gingival cells compared to only EA.

Although the score-based method allowed determining the real effectiveness of the included studies, the mechanical stability of the TiO_2 layer needs to be further elucidated before clinical investigation in humans. Lastly, it is important to add that although biofilm formation and bacterial adhesion were not the subjects of the present review, EA surfaces may also affect microbial colonization and biofilm formation.

Author Contributions: Conceptualization, M.-J.C. and O.F.; methodology, M.-J.C., E.M. and O.F.; software, M.-J.C.; validation, P.P. and P.D. and O.F.; writing—original draft preparation, M.-J.C.; supervision, O.F. and N.L. All authors have read and agreed to the published version of the manuscript.

Funding: This research received no external funding.

Institutional Review Board Statement: Not applicable.

Informed Consent Statement: Not applicable.

Acknowledgments: The authors would like to thank Karan Gulati, who generously gave images from his research, and Corinne Dupuy and Pierre-Augustin Crenn for the design of the 3D images.

Conflicts of Interest: The authors declare no conflict of interest.

References

1. Corvino, E.; Pesce, P.; Mura, R.; Marcano, E.; Canullo, L. Influence of Modified Titanium Abutment Surface on Peri-implant Soft Tissue Behavior: A Systematic Review of In Vitro Studies. *Int. J. Oral Maxillofac. Implant.* **2020**, *35*, 503–519. [CrossRef]
2. Canullo, L.; Annunziata, M.; Pesce, P.; Tommasato, G.; Nastri, L.; Guida, L. Influence of abutment material and modifications on peri-implant soft-tissue attachment: A systematic review and meta-analysis of histological animal studies. *J. Prosthet. Dent.* **2021**, *125*, 426–436. [CrossRef]
3. Guo, T.; Gulati, K.; Arora, H.; Han, P.; Fournier, B.; Ivanovski, S. Orchestrating soft tissue integration at the transmucosal region of titanium implants. *Acta Biomater.* **2021**, *124*, 33–49. [CrossRef] [PubMed]
4. Macak, J.M.; Tsuchiya, H.; Taveira, L.; Ghicov, A.; Schmuki, P. Self-organized nanotubular oxide layers on Ti-6Al-7Nb and Ti-6Al-4V formed by anodization in NH4F solutions. *J. Biomed. Mater. Res.* **2005**, *75*, 928–933. [CrossRef] [PubMed]
5. Demetrescu, I.; Pirvu, C.; Mitran, V. Effect of nano-topographical features of Ti/TiO(2) electrode surface on cell response and electrochemical stability in artificial saliva. *Bioelectrochemistry Amst. Neth* **2010**, *79*, 122–129. [CrossRef]
6. Kunrath, M.F.; Diz, F.M.; Magini, R.; Galárraga-Vinueza, M.E. Nanointeraction: The profound influence of nanostructured and nano-drug delivery biomedical implant surfaces on cell behavior. *Adv. Colloid. Interface Sci.* **2020**, *284*, 102265. [CrossRef] [PubMed]
7. Page, M.J.; McKenzie, J.E.; Bossuyt, P.M.; Boutron, I.; Hoffmann, T.C.; Mulrow, C.D.; Shamseer, L.; Tetzlaff, J.M.; Akl, E.A.; Brennan, S.E.; et al. The PRISMA 2020 statement: An updated guideline for reporting systematic reviews. *J. Clin. Epidemiol.* **2021**, *134*, 178–189. [CrossRef] [PubMed]
8. Wang, C.; Wang, X.; Lu, R.; Gao, S.; Ling, Y.; Chen, S. Responses of human gingival fibroblasts to superhydrophilic hydrogenated titanium dioxide nanotubes. *Colloids Surf. B Biointerfaces* **2021**, *198*, 111489. [CrossRef] [PubMed]
9. Gulati, K.; Moon, H.-J.; Kumar, P.T.S.; Han, P.; Ivanovski, S. Anodized anisotropic titanium surfaces for enhanced guidance of gingival fibroblasts. *Mater. Sci. Eng. C Mater. Biol. Appl.* **2020**, *112*, 110860. [CrossRef]
10. Xu, Z.; He, Y.; Zeng, X.; Zeng, X.; Huang, J.; Lin, X.; Chen, J. Enhanced Human Gingival Fibroblast Response and Reduced Porphyromonas gingivalis Adhesion with Titania Nanotubes. *BioMed Res. Int.* **2020**, 5651780. [CrossRef] [PubMed]
11. Zheng, X.; Sun, J.; Li, W.; Dong, B.; Song, Y.; Xu, W.; Zhou, Y.; Wang, L. Engineering nanotubular titania with gold nanoparticles for antibiofilm enhancement and soft tissue healing promotion. *J. Electroanal. Chem. B* **2020**, *871*, 114362. [CrossRef]
12. Llopis-Grimalt, M.A.; Amengual-Tugores, A.M.; Monjo, M.; Ramis, J.M. Oriented Cell Alignment Induced by a Nanostructured Titanium Surface Enhances Expression of Cell Differentiation Markers. *Nanomaterials* **2019**, *9*, 1661. [CrossRef]
13. Wang, J.; He, X.-T.; Xu, X.-Y.; Yin, Y.; Li, X.; Bi, C.-S.; Hong, Y.-L.; Chen, F.-M. Surface modification via plasmid-mediated pLAMA3-CM gene transfection promotes the attachment of gingival epithelial cells to titanium sheets in vitro and improves biological sealing at the transmucosal sites of titanium implants in vivo. *J. Mater. Chem. B* **2019**, *7*, 7415–7427. [CrossRef] [PubMed]
14. Ferrà-Cañellas, M.D.M.; Llopis-Grimalt, M.A.; Monjo, M.; Ramis, J.M. Tuning Nanopore Diameter of Titanium Surfaces to Improve Human Gingival Fibroblast Response. *Int. J. Mol. Sci.* **2018**, *19*, 2881. [CrossRef]

15. Nojiri, T.; Chen, C.-Y.; Kim, D.M.; Da Silva, J.; Lee, C.; Maeno, M.; McClelland, A.A.; Tse, B.; Ishikawa-Nagai, S.; Hatakeyama, W.; et al. Establishment of perpendicular protrusion of type I collagen on TiO2 nanotube surface as a priming site of peri-implant connective fibers. *J. Nanobiotechnology* **2019**, *17*, 34. [CrossRef] [PubMed]
16. Gulati, K.; Moon, H.-J.; Li, T.; Kumar, P.S.; Ivanovski, S. Titania nanopores with dual micro-/nano-topography for selective cellular bioactivity. *Mater. Sci. Eng. C Mater. Biol. Appl.* **2018**, *91*, 624–630. [CrossRef] [PubMed]
17. Xu, R.; Hu, X.; Yu, X.; Wan, S.; Wu, F.; Ouyang, J.; Deng, F. Micro-/nano-topography of selective laser melting titanium enhances adhesion and proliferation and regulates adhesion-related gene expressions of human gingival fibroblasts and human gingival epithelial cells. *Int. J. Nanomed.* **2018**, *13*, 5045–5057. [CrossRef]
18. Liu, X.; Zhou, X.; Li, S.; Lai, R.; Zhou, Z.; Zhang, Y.; Zhou, L. Effects of titania nanotubes with or without bovine serum albumin loaded on human gingival fibroblasts. *Int. J. Nanomed.* **2014**, *9*, 1185–1198. [CrossRef]
19. Guida, L.; Oliva, A.; Basile, M.A.; Giordano, M.; Nastri, L.; Annunziata, M. Annunziata. Human gingival fibroblast functions are stimulated by oxidized nano-structured titanium surfaces. *J. Dent.* **2013**, *41*, 900–907. [CrossRef]
20. Zhang, Y.; Ma, Q.; Chu, P.; Mei, S.; Ji, K.; Jin, L. Concentration- and time-dependent response of human gingival fibroblasts to fibroblast growth factor 2 immobilized on titanium dental implants. *Int. J. Nanomed.* **2012**, *7*, 1965–1976. [CrossRef]
21. Ma, Q.; Mei, S.; Ji, K.; Zhang, Y.; Chu, P.K. Immobilization of Ag nanoparticles/FGF-2 on a modified titanium implant surface and improved human gingival fibroblasts behavior. *J. Biomed. Mater. Res. A* **2011**, *98*, 274–286. [CrossRef]
22. Guo, T.; Oztug, N.A.K.; Han, P.; Ivanovski, S.; Gulati, K. Old is Gold: Electrolyte Aging Influences the Topography, Chemistry, and Bioactivity of Anodized TiO2 Nanopores. *ACS Appl. Mater. Interfaces* **2021**, *13*, 7897–7912. [CrossRef] [PubMed]
23. Guo, T.; Oztug, N.A.K.; Han, P.; Ivanovski, S.; Gulati, K. Influence of sterilization on the performance of anodized nanoporous titanium implants. *Mater. Sci. Eng. C* **2021**, *130*, 112429. [CrossRef]
24. Zhao, L.; Mei, S.; Wang, W.; Chu, P.K.; Wu, Z.; Zhang, Y. The role of sterilization in the cytocompatibility of titania nanotubes. *Biomaterials* **2010**, *31*, 2055–2063. [CrossRef]
25. Subramani, K.; Jung, R.E.; Molenberg, A.; Hammerle, C.H.F. Biofilm on dental implants: A review of the literature. *Int. J. Oral Maxillofac. Implant.* **2009**, *24*, 616–626.
26. Fu, Y.; Mo, A. A Review on the Electrochemically Self-organized Titania Nanotube Arrays: Synthesis, Modifications, and Biomedical Applications. *Nanoscale Res. Lett.* **2018**, *13*, 187. [CrossRef]
27. Kafshgari, M.H.; Goldmann, W.H. Insights into Theranostic Properties of Titanium Dioxide for Nanomedicine. *Nano-Micro Lett.* **2020**, *12*, 22. [CrossRef]
28. McNamara, L.E.; Sjöström, T.; Seunarine, K.; Meek, R.D.; Su, B.; Dalby, M.J. Investigation of the limits of nanoscale filopodial interactions. *J. Tissue Eng.* **2014**, *5*, 2041731414536177. [CrossRef]
29. Mohamed, A.E.R.; Kasemphaibulsuk, N.; Rohani, S.; Barghi, S. Fabrication of titania nanotube arrays in viscous electrolytes. *J. Nanosci. Nanotechnol.* **2010**, *10*, 1998–2008. [CrossRef] [PubMed]
30. Kearns, V.R.; Williams, R.L.; Mirvakily, F.; Doherty, P.J.; Martin, N. Guided gingival fibroblast attachment to titanium surfaces: An in vitro study. *J. Clin. Periodontol.* **2013**, *40*, 99–108. [CrossRef] [PubMed]
31. Gristina, A.G. Biomaterial-centered infection: Microbial adhesion versus tissue integration. *Science* **1987**, *237*, 1588–1595. [CrossRef] [PubMed]
32. Guo, T.; Gulati, K.; Arora, H.; Han, P.; Fournier, B.; Ivanovski, S. Race to invade: Understanding soft tissue integration at the transmucosal region of titanium dental implants. *Dent. Mater.* **2021**, *37*, 816–831. [CrossRef] [PubMed]